

2012

Inducing extended line defects in graphene by linear adsorption of C and N atoms

Yu Li

Department of Physics, University of Science and Technology of China, Hefei, China

Rui-Qin Zhang

Department of Physics and Materials Science, City University of Hong Kong, Hong Kong SAR, China

Zijing Lin

Department of Physics, University of Science and Technology of China, Hefei, China

Michel Andre Van Hove

Hong Kong Baptist University, vanhove@hkbu.edu.hk

This document is the authors' final version of the published article.

Link to published article: <http://dx.doi.org/10.1063/1.4772212>

APA Citation

Li, Y., Zhang, R., Lin, Z., & Van Hove, M. (2012). Inducing extended line defects in graphene by linear adsorption of C and N atoms. *Applied Physics Letters*, 101 (25), 253105-1-253105-4. <https://doi.org/10.1063/1.4772212>

This Journal Article is brought to you for free and open access by the Research Institutes, Centres and Administrative Units at HKBU Institutional Repository. It has been accepted for inclusion in Institute of Computational and Theoretical Studies by an authorized administrator of HKBU Institutional Repository. For more information, please contact repository@hkbu.edu.hk.

Inducing extended line defects in graphene by linear adsorption of C and N atoms

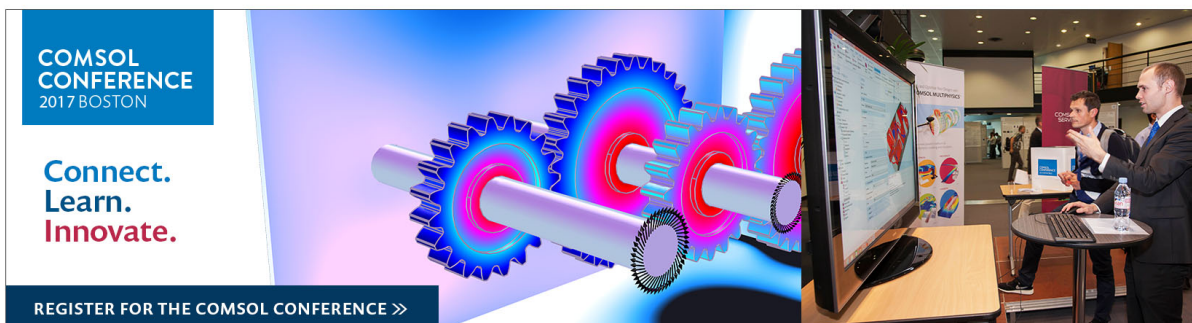
Yu Li, , Rui-Qin Zhang, , Zijing Lin, and , and Michel A. Van Hove

Citation: *Appl. Phys. Lett.* **101**, 253105 (2012); doi: 10.1063/1.4772212

View online: <http://dx.doi.org/10.1063/1.4772212>

View Table of Contents: <http://aip.scitation.org/toc/apl/101/25>

Published by the [American Institute of Physics](#)



Inducing extended line defects in graphene by linear adsorption of C and N atoms

Yu Li,^{1,2,3} Rui-Qin Zhang,^{2,a)} Zijin Lin,^{1,a)} and Michel A. Van Hove^{4,a)}

¹*Department of Physics, University of Science and Technology of China, Hefei, China*

²*Department of Physics and Materials Science, City University of Hong Kong, Hong Kong SAR, China*

³*USTC-CityU Joint Advanced Research Centre, Suzhou 215123, China*

⁴*Institute of Computational and Theoretical Studies & Department of Physics, Hong Kong Baptist University, Hong Kong SAR, China*

(Received 14 October 2012; accepted 30 November 2012; published online 17 December 2012)

We propose a possible approach for controlled formation of various 585 (containing pentagonal and octagonal carbon rings) extended line defects (ELDs) by linear adsorption of various kinds of atoms (C, N, B, O) on a graphene substrate, based upon density functional theory and molecular-dynamics (MD) simulations. We find out that the C and N atoms spontaneously transform to 585 ELDs while other elements find specific stable configurations. To confirm the feasibility of forming the ELD from line adsorption, investigation of the critical transformation conditions of the 585 ELD is involved based upon various adsorption models and adsorption densities. © 2012 American Institute of Physics. [<http://dx.doi.org/10.1063/1.4772212>]

Graphene as a potential candidate for fascinating physical and chemical applications has attracted a great deal of research and exploration ever since the isolation of free-standing graphene in 2004.^{1,2} Various types of defects in graphene which may result in nanostructures exhibiting fascinating electronic properties open a broad range of potential applications.^{3–12} Hypothetical one-dimensional-defect structures embedded in graphene and carbon nanotubes have been suggested from computer modeling.^{13–16} A recent experimental realization of a type of extended line defect (585 ELD¹⁷) has triggered a “gold rush” for the scientific interest of such derivatives. Hereafter, recently the focus of research in defected graphene has moved from point defects to extended line defects. In contrast to the numerous subsequent studies on the electronic and magnetic properties of the ELD–graphene system, the number of theoretical and experimental reports on formation methods of ELDs is limited. The only experimental realization of a 585 like ELD reported recently was formed by spontaneous reconstruction of two different adsorption sublattices during growth on a nickel substrate.¹⁷ This formation mechanism of introducing the 585 ELD as grain boundaries has been investigated theoretically as a growth fault or stacking fault,¹⁶ but experimentally only the pure C ELD system could be formed, showing a high dependency on experimental conditions such as the presence and nature of a substrate. Certain other possible pathways, such as implantation of C₂ clusters in the perfect lattice¹⁸ and thermal annealing of the system with an array of atomic divacancies,¹⁴ have also been proposed to form ELDs but without detailed exploration. A more generalized means of forming various types of ELDs, for example, using foreign elements (doped ELD), is quite demanding.

The purpose of this paper is to suggest a possible approach for controlled formation of various 585 ELDs

based upon density functional theory (DFT) and molecular-dynamics (MD) simulations. Our DFT results clearly show that linear adsorption of foreign adatoms can form a 585 ELD as well as a N-doping 585 ELD at favored adsorption density and temperature. The sequential adsorption pattern also plays an important role in the reconstruction process considering possible diffusion and coalescence. Our finding is a discovery of applying linear adsorption to form 585 ELD families in graphene and should favor the robust exploration of this area.

Adsorption, as a widely used and confirmed technology, is expected to induce useful modifications of electronic properties of carbon based materials.^{19–22} The most frequently considered form of adsorption is locally isolated with high stability and without evident additional defects induced in the host lattice. Multiple adsorptions have been rarely considered due to the complication and underestimation of their profound applications.²³ Interestingly, multiple adsorptions may influence the substrate strongly and sometimes may lead to reconstruction of the host lattice. Our research reveals that a high density of adatoms can significantly destroy the intrinsic lattice of graphene by coalescing into the host and forming a different type of lattice structure as grain boundary. The array of adatoms can be achieved by preferential sticking into specific adsorbate structures and points to a possible route to ELD formation.

We used the Troullier-Martins pseudopotential²⁴ with the generalized gradient approximation (GGA) (Perdew-Burke-Ernzerhof²⁵ functional) for the density functional theory as implemented in the SIESTA^{26,27} package, with inclusion of spin polarization and an energy mesh cutoff of 250 Ry. As widely studied, the bridge site is the most stable configuration for isolated C and N adatoms on graphene.^{21,22} A supercell of intrinsic graphene upon which adatoms array linearly at the bridge sites is used as our representative model (see Figure 1(a)), with a vacuum layer of 10 Å in perpendicular to the graphene sheet. A 10 × 10 × 1 k-point mesh for Brillouin zone sampling is used and the convergence for the

^{a)}Authors to whom correspondence should be addressed. Electronic addresses: aprqz@cityu.edu.hk; zjlin@ustc.edu.cn; and vanhove@hkbu.edu.hk.

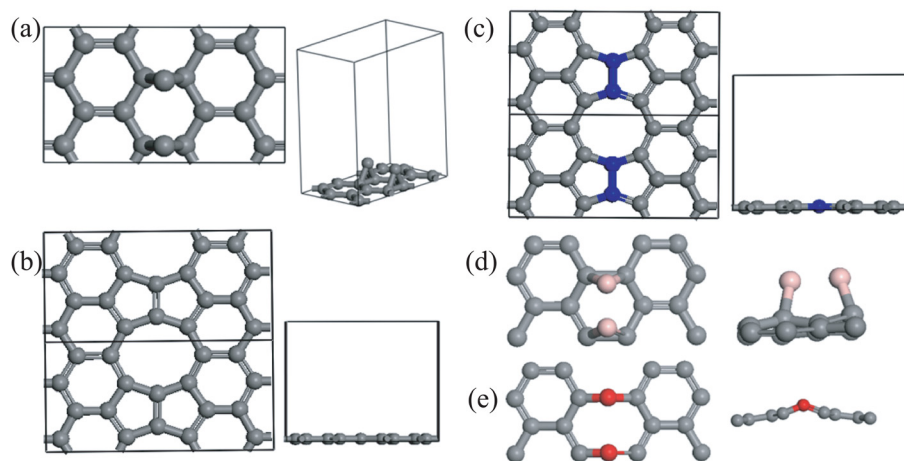


FIG. 1. Top and side views of initial and optimized structures of interest (rectangles show unit cells used in the calculations): (a) model of C linear adsorption on graphene (similar initial models apply for all other elements: N, B and O) and (b) optimized 585 ELD, (c) optimized N-585 ELD, (d) optimized B linear adsorption on graphene within a unit cell, and (e) optimized O linear adsorption on graphene within a unit cell.

forces is set to be 0.02 eV/\AA . Not only C atoms but also N, B, and O atoms are studied, whose contrasting behaviors give useful indications for experimental applications.

After our model structural optimizations (Figures 1(b) and 1(c)), the C and N adatoms are incorporated into the graphene lattice, which reconstructs into the 585 ELD structure and a doped N-585 ELD structure, respectively. By carefully analyzing the reconstruction, we observe that the adatoms (initial C-C (N-N) distance is $\sim 2.4 \text{ \AA}$) directly bond to each other until a final relaxed bond length $\sim 1.44 \text{ \AA}$. In the process, they induce such a strong repulsion among underlying C-C atoms in the graphene lattice that some C-C bonds are broken. Then, the adatoms move into and finally embed themselves within the planar lattice. During this process, certain C-C bond rotations favor accommodating the adatoms and reconstruct as 585 ELD. This ELD reconstruction is ascribed to the strong tension induced by the obvious bonding between the adatoms (bond length $\sim 1.44 \text{ \AA}$). The band gap of N-585 ELD is around 0.6 eV , in contrast to the metallic property of C-585 ELD. Obviously, such a linear adsorption route can generate a family of doping-585 ELDs in graphene exhibiting broad electronic structures, which provides potential applications in designing various nano-devices.

In comparison to C and N reconstruction, O, B, Si, S, P, Cl adatoms fail to be incorporated into the graphene lattice to form ELDs. As shown in Figure 1(e), the O adatoms break nearby C-C bonds but remain as a bulge outside of the plane. The overall geometry is similar to the isolated oxygen adsorption geometry²⁸ but with a stronger repulsion in the underlying C-C bonds. The absence of ELD reconstruction in the O adsorption system is due to the nonbonding character (large distance $\sim 2.5 \text{ \AA}$) between the O adatoms and suggests that strong bonding between adatoms is a critical character of inducing reconstruction of ELD. In particular, by stacking two O-linear-adsorption graphene layers face to face (with the O bulges pointing outward), an O-doped carbon nanotube can be realized spontaneously, based upon our MD simulations. The B adsorption system confirms the importance of bonding between adatoms: the B adatoms get closer ($\sim 1.8 \text{ \AA}$) as compared to the O case but still maintain a bridge adsorption geometry due to weak B-B interaction (Figure 1(d)). By contrast, the B-585-ELD structure is locally stable with $\sim 0.23 \text{ eV/atom}$ lower than the adsorption

geometry (Figure 1(d)). It is expected to transform between the two local minima in favorable conditions if the activation barrier is overcome. Consequently, the B-585-ELD in graphene may also be achieved by this route.

To confirm the feasibility of this linear adsorption reconstruction route, investigation of the critical transformation conditions of such 585 ELD should be conducted with close attention to possible adsorption densities and patterns. First, we focus on the role of adsorption densities within the linear adsorption configuration (the adsorption density is defined as the ratio of the number of adatoms to the overall number of bridge sites within a line). The coverage of adatoms ranges from 50% (Figure 2(a)) and 75% (Figure 2(c)), to 100% (Figure 1(a)). We find that C adatom dimers (50%) succeed in spontaneously embedding themselves into the graphene lattice and form 7557 defects as shown in Figure 2(b). This transformation occurs at a relatively low density indicating a higher probability of inducing C-585 ELD by multiple adsorptions. At an increased density as shown in Figure 2(d), a 5885-like ELD forms, considered as an evolutionary phase of the 50% system with more C atoms falling onto the graphene surface.

As compared to the strong ability of C adatoms to reconstruct into 585-ELD, it is relatively complicated for N adatoms. The relaxed N dimers on graphene (50%, Figure 2(e)) maintain a bridge adsorption geometry connected with single bonds (bond length of 1.51 \AA) between each other. Considering the possible coalescence of N adatoms into molecules, the stability of this optimized geometry has been tested by MD simulation at various temperatures. Though remaining stable below 200 K , the dimers form N_2 molecules and physically adsorb on the graphene surface at 300 K . Nevertheless, at low temperatures, the 50% N-adsorbed system can exist long enough to develop to higher density (75%), which evolves to form an 8557-ELD structure (see Figure 2(f)). The stability of this 8557-ELD has been confirmed by MD simulation at 400 K , proving that it serves as a precursor to forming the 585-ELD only if more N ions enter the system.

Admittedly, the experimental situation is always more complicated due to various possibilities of adsorption patterns and evolutions of adatoms. In addition to the above mentioned density dependence, the energetic preference of the linear pattern should be taken into account. Therefore, several plausible configurations for dimer adsorptions (the

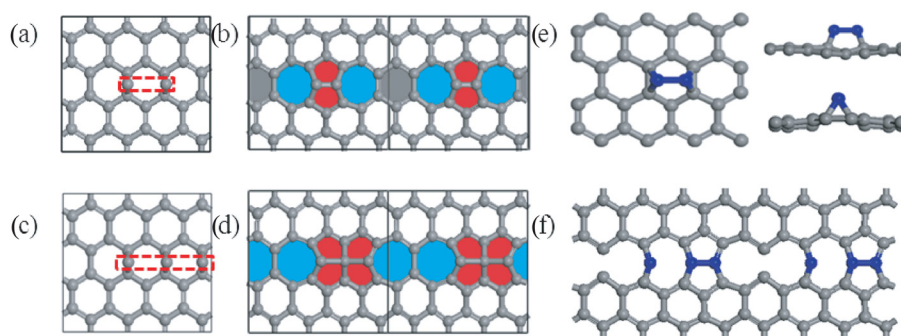


FIG. 2. Designed models and optimized structures for C and N linear adsorption on graphene at various densities. (a) and (c) Top views of the initial model within one unit cell (the adatoms are outlined by red dashed rectangles); the adsorption density is (a) 50%, resp. (c) 75%. The optimized C-ELD structures are shown in supercells doubled in size along the ELD direction: (b) 50% and (d) 75% (the pentagonal rings are colored red, the heptagonal rings blue, and the hexagonal rings in the ELD direction grey). The optimized structures of the N system are shown in: (e) 50% within a unit cell and (f) 75% within doubled supercells in the ELD direction. The two insets in (e) show two lateral views of a B-B pair.

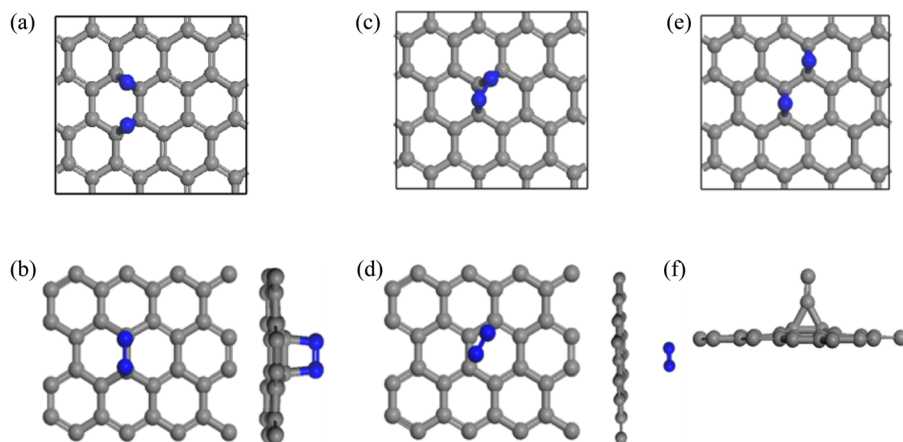


FIG. 3. Three dimer adsorption patterns on graphene: (a) the next-neighbor N dimer or *arm* dimer and (b) its optimized configuration, (c) the *near-neighbor* N dimer and (d) its optimized configuration, and (e) the *parallel* N dimers. (f) Stable configuration for C dimers on graphene with *arm*, *near-neighbor*, and *parallel* dimers patterns.

arm, *next-neighbour*, and *parallel* dimers in Figure 3 are studied as energetically competing geometries of the linear structure.

Figure 3 illustrates the initial and optimized structures of these configurations. The *arm* dimer (Figure 3(a)) forms N-N bond and transforms to top sites as shown in Figure 3(b). The *next-neighbor* pattern (Figure 3(c)) is unstable due to the close initial distance within the dimer: a N_2 molecule forms directly and physically adsorbs on graphene after relaxation (Figure 3(d), physical adsorption). Conversely, the *parallel* dimers (Figure 3(e)) maintain their initial geometry after relaxation and have the highest total energy as shown in Table I. The migration barrier of N adatom on graphene is ~ 1.00 eV,²⁹ which means that N adatoms should be highly mobile at high temperatures but of limited mobility at room temperatures. Therefore, we recognize that the parallel pattern is thermally stable at room temperature but has poor energetic priority.

From Table I, the *arm* pattern possesses a lower total energy than the linear pattern by 2.26 eV and seems more stable. However, in the N system, the coalescence of adatoms occurs more frequently than diffusion with a reported activation barrier of 0.8 eV.³⁰ At some temperature, the stability of these two systems depends more on the barrier of coalescence. It is reasonable that the *arm* dimer favors the coalescence reaction over the linear dimer, according to an easy bonding character analysis. The N atoms in the *next-neighbor* pattern make a double bond between each other and single

bonds with the C atoms in graphene according to our optimization, and will coalesce to form a molecule above 300 K as indicated by MD simulations. The linear configuration has a single bond between N atoms but two C-N single bonds for each adatom. When coalescence happens, the *parallel* configuration only needs to break one C-N bond for each N, in contrast to the two C-N bonds for each N in the linear dimer situation. Obviously, the lower total energy of the *parallel* dimer as compared to the linear dimer is due to the stronger bonding between the N adatoms (a double bond) instead of the interaction with the substrate. Hereafter, a critical temperature exists to maintain the linear configuration while removing other dimer configurations. Admittedly, the exact condition to keep the linear pattern instead of the *arm* pattern is difficult to determine theoretically, but such qualitative stability preference is reasonable to support our assumption.

The energy preference between various adsorption patterns is more direct in the C-graphene system. As shown in

TABLE I. The relative total energies of some typical N dimer adsorptions on graphene.

Dimer pattern ^a	Linear	Next-neighbor	Arm	Parallel
Energy ^b (eV)	6.44	0	4.18	7.58

^aThe linear geometry is shown in Fig. 1, while the three other geometries are shown in Fig. 3.

^bThe energy of the next-neighbor dimer is set as reference (0 eV).

Figure 3(f), all the designed configurations of C dimers (except for the linear adsorption geometry) on graphene present clustering of adatoms after relaxation, with a less favorable energy ~ 0.4 eV higher than that of the 585-ELD structure shown in Figure 1(b). Therefore, the reconstruction of C-585 ELD is highly preferred from the standpoint of stability and hence should occur spontaneously in experiment. The migration barrier of C adatoms on pure graphene is only ~ 0.25 eV,²⁹ so that C atoms can migrate easily and rapidly at room temperature. The rapid diffusion of C adatoms is expected to favor the reconstruction in experiment.

In summary, using the linear adsorption of C and N adatoms on graphene, we induce 585 ELD structures as well as N doped 585 ELD structures in the pure graphene lattice. We demonstrate that the 585 ELD can be reconstructed spontaneously at favorable temperatures and adsorption densities. We find that coalescence of N₂ molecules plays an important role in the N system, which reduces the possibility of reconstruction into ELD in experiment. While for the pure C system, the adatoms show a high tendency of embedding into the graphene sheet. Our work is expected to simulate experiments as a potential mechanism of introducing the doped 585-ELD family with various electronic properties favoring wide applications.

The work described in this paper was supported in part by a grant from the Research Grants Council of Hong Kong SAR [Project No. CityU 103511], by the State Key Development Program for Basic Research of China (Grant No. 2012CB215405), by the National Natural Science Foundation of China (Grant No. 11074233), and by the High Performance Cluster Computing Centre, Hong Kong Baptist University, which receives funding from Research Grants Council, University Grants Committee of the HKSAR, and Hong Kong Baptist University.

¹K. S. Novoselov, A. K. Geim, S. V. Morozov, D. Jiang, Y. Zhang, S. V. Dubonos, I. V. Grigorieva, and A. A. Firsov, *Science* **306**(5696), 666 (2004).

²K. S. Novoselov, D. Jiang, F. Schedin, T. J. Booth, V. V. Khotkevich, S. V. Morozov, and A. K. Geim, *Proc. Natl. Acad. Sci. U.S.A.* **102**(30), 10451 (2005).

³C. Cao, L. N. Chen, D. Zhang, W. R. Huang, S. S. Ma, and H. Xu, *Solid State Commun* **152**(1), 45 (2012).

⁴C. C. Ma, X. H. Shao, and D. P. Cao, *J. Mater. Chem.* **22**(18), 8911 (2012).

⁵C. Wang, X. J. Han, P. Xu, X. L. Zhang, Y. C. Du, S. R. Hu, J. Y. Wang, and X. H. Wang, *Appl. Phys. Lett.* **98**(7), 072906 (2011).

⁶Y. H. Zhang, K. G. Zhou, X. C. Gou, K. F. Xie, H. L. Zhang, and Y. Peng, *Chem. Phys. Lett.* **484**(4–6), 266 (2010).

⁷Y. P. Zheng, L. Q. Xu, Z. Y. Fan, N. Wei, Y. Lu, and Z. G. Huang, *Curr. Nanosci.* **8**(1), 89 (2012).

⁸M. Bagge-Hansen, R. A. Outlaw, M. Y. Zhu, H. J. Chen, and D. M. Manos, *J. Vac. Sci. Technol. B* **27**(6), 2413 (2009).

⁹V. M. Bermudez and J. T. Robinson, *Langmuir* **27**(17), 11026 (2011).

¹⁰Y. C. Chang and S. Haas, *Phys. Rev. B* **83**(8), 085406 (2011).

¹¹P. Y. Huang, C. S. Ruiz-Vargas, A. M. van der Zande, W. S. Whitney, M. P. Levendorf, J. W. Kevek, S. Garg, J. S. Alden, C. J. Hustedt, Y. Zhu, J. Park, P. L. McEuen, and D. A. Muller, *Nature* **469**(7330), 389 (2011).

¹²L. Z. Kou, C. Tang, W. L. Guo, and C. F. Chen, *ACS Nano* **5**(2), 1012 (2011).

¹³A. R. Botello-Mendez, E. Cruz-Silva, F. Lopez-Urias, B. G. Sumpter, V. Meunier, M. Terrones, and H. Terrones, *ACS Nano* **3**(11), 3606 (2009).

¹⁴S. Okada, K. Nakada, K. Kuwabara, K. Daigoku, and T. Kawai, *Phys. Rev. B* **74**(12), 121412(R) (2006).

¹⁵Y. Li, R. Q. Zhang, Z. Lin, and M. A. Van Hove, *Nanoscale* **4**(8), 2580 (2012).

¹⁶M. U. Kahaly, S. P. Singh, and U. V. Waghmare, *Small* **4**(12), 2209 (2008).

¹⁷J. Lahiri, Y. Lin, P. Bozkurt, I. I. Oleynik, and M. Batzill, *Nat. Nanotechnol.* **5**(5), 326 (2010).

¹⁸S. Okada, K. Nakada, and T. Kawai, *J. Phys.: Condens. Matter* **19**(36), 365231 (2007).

¹⁹B. Huang, Z. Y. Li, Z. R. Liu, G. Zhou, S. G. Hao, J. Wu, B. L. Gu, and W. H. Duan, *J. Phys. Chem. C* **112**(35), 13442 (2008).

²⁰S. Y. Davydov and G. I. Sabirova, *Tech. Phys. Lett.* **36**(12), 1154 (2010).

²¹E. Kan, H. J. Xiang, F. Wu, C. Lee, J. L. Yang, and M. H. Whangbo, *Appl. Phys. Lett.* **96**(10), 102503 (2010).

²²S. S. Yu, W. T. Zheng, and Q. Jiang, *IEEE Trans. Nanotechnol.* **9**(2), 243 (2010).

²³S. Casolo, O. M. Lovvik, R. Martinazzo, and G. F. Tantardini, *J. Chem. Phys.* **130**(5), 054704 (2009).

²⁴N. Troullier and J. L. Martins, *Phys. Rev. B* **43**(3), 1993 (1991).

²⁵J. P. Perdew, K. Burke, and M. Ernzerhof, *Phys. Rev. Lett.* **77**(18), 3865 (1996); J. P. Perdew, K. Burke, and M. Ernzerhof, *Phys. Rev. Lett.* **78**(7), 1396 (1997).

²⁶P. Ordejón, E. Artacho, and J. M. Soler, *Phys. Rev. B* **53**(16), R10441 (1996).

²⁷J. M. Soler, E. Artacho, J. D. Gale, A. Garcia, J. Junquera, P. Ordejón, and D. Sanchez-Portal, *J. Phys.: Condens. Matter* **14**(11), 2745 (2002).

²⁸D. C. Sorescu, K. D. Jordan, and P. Avouris, *J. Phys. Chem. B* **105**(45), 11227 (2001).

²⁹K. Nakada and A. Ishii, *Solid State Commun* **151**(1), 13 (2011).

³⁰Y. C. Ma, A. S. Foster, A. V. Krashennnikov, and R. M. Nieminen, *Phys. Rev. B* **72**(20), 205416 (2005).